4244 *Biochemistry* **2010,** *49,* 4244–4254
DOI: 10.1021/bi1001213

BIOCHEMISTRY
including biophysical chemistry & molecular biology
Article

Identification and Inhibitory Properties of a Novel Ca^{2+}/Calmodulin Antagonist†

Josep Colomer,‡ Allison A. Schmitt,§ Eric J. Toone,§ and Anthony R. Means*,‡

‡*Department of Pharmacology and Cancer Biology, Duke University Medical Center, P.O. Box 3813, Durham, North Carolina 27710, and* §*Department of Chemistry, Duke University, P.O. Box 90317, Durham, North Carolina 27708*

Received January 26, 2010; Revised Manuscript Received April 9, 2010

ABSTRACT: We developed a high-throughput yeast-based assay to screen for chemical inhibitors of Ca^{2+}/calmodulin-dependent kinase pathways. After screening two small libraries, we identified the novel antagonist 125-C9, a substituted ethyleneamine. In vitro kinase assays confirmed that 125-C9 inhibited several calmodulin-dependent kinases (CaMKs) competitively with Ca^{2+}/calmodulin (Ca^{2+}/CaM). This suggested that 125-C9 acted as an antagonist for Ca^{2+}/CaM rather than for CaMKs. We confirmed this hypothesis by showing that 125-C9 binds directly to Ca^{2+}/CaM using isothermal titration calorimetry. We further characterized binding of 125-C9 to Ca^{2+}/CaM and compared its properties with those of two well-studied CaM antagonists: trifluoperazine (TFP) and W-13. Isothermal titration calorimetry revealed that binding of 125-C9 to CaM is absolutely Ca^{2+}-dependent, likely occurs with a stoichiometry of five 125-C9 molecules to one CaM molecule, and involves an exchange of two protons at pH 7.0. Binding of 125-C9 is driven overall by entropy and appears to be competitive with TFP and W-13, which is consistent with occupation of similar binding sites. To test the effects of 125-C9 in living cells, we evaluated mitogen-stimulated re-entry of quiescent cells into proliferation and found similar, although slightly better, levels of inhibition by 125-C9 than by TFP and W-13. Our results not only define a novel Ca^{2+}/CaM inhibitor but also reveal that chemically unique CaM antagonists can bind CaM by distinct mechanisms but similarly inhibit cellular actions of CaM.

Calcium (Ca^{2+}) is a major cell signaling transducer that links cell stimuli to specific cell responses. A 10-fold increase in cytoplasmic Ca^{2+} levels from 100 nM to 1 μM is a common response to a variety of cell stimuli, resulting in Ca^{2+} binding to a variety of calcium binding proteins (*1*). One of the most prominent calcium binding proteins is calmodulin (CaM),[1] which is evolutionarily conserved among all eukaryotic organisms. CaM contains four Ca^{2+} binding EF-hand motifs and undergoes conformational changes upon binding of four Ca^{2+} molecules. Consequently, two hydrophobic domains of CaM become exposed to the solvent, one on the N-terminal domain and one on the C-terminal domain, markedly increasing the affinity of Ca^{2+}/CaM for many Ca^{2+}/CaM binding proteins. This increased affinity leads to CaM binding and regulation of protein function in a Ca^{2+}-dependent manner (reviewed in ref *2*), resulting in the transduction of the Ca^{2+} signal into specific functions in the cell. Because ~300 CaM-binding proteins have been described to date (*3*), the range of Ca^{2+} functions in the cell is very broad.

Previous work from our laboratory has shown that a pathway regulated by the Ca^{2+}/CaM-dependent enzyme kinase kinase β (CaMKKβ) in cells of the arcuate nucleus in the hypothalamus is necessary for the synthesis and release of NPY and AgRP factors that primarily regulate appetite (*4*). The Ca^{2+}/CaM/CaMKKβ signaling pathway regulates this process by phosphorylating and activating AMPK, a holoenzyme that consists of three subunits named α (catalytic), β, and γ (regulatory). The γ subunit confers AMP sensitivity to the enzyme complex, resulting in holoenzyme activation. The α subunit must be phosphorylated at T172 to confer maximum activity to the complex (*5*). Three different kinases in mammals can phosphorylate and activate α-AMPK: LKB1, TAK1, and CaMKKβ (*6*−*8*). However, in cells of the arcuate nucleus, Ca^{2+}/CaM/CaMKKβ complexes only with the α and β subunits of AMPK, turning an otherwise AMP sensitive enzyme into a Ca^{2+} sensitive enzyme (*4*).

Like CaM, AMPK is evolutionarily conserved in all eukaryotic organisms from yeast to mammals (*9*). Yeast cells express subunits equivalent to α-AMPK (snf1), β-AMPK (Sip1, Sip2, Gal83), and γ-AMPK (snf4). AMPK activation is required for yeast to grow on media in which glucose is replaced by a different type of carbon source (raffinose, for example) (*10*). In addition, snf1 must be phosphorylated at T210 (equivalent to T172 in mammalian α-AMPK), and such phosphorylation is catalyzed by one of the three yeast snf1 activators: Sak1, Tos3, and Elm1 (*11*, *12*). This pathway is so well conserved that any mammalian activator of AMPK (LKB1, TAK1, or CaMKKβ) can substitute for all three yeast activators (*7*, *13*, *14*) (Figure 1A).

On the basis of these similarities, we designed a strategy to identify inhibitors of the Ca^{2+}/CaM/CaMKKβ pathway in yeast. We substituted either a mammalian CaM-dependent kinase (CaMKKβ) or a CaM- independent kinase (TAK1) for the yeast snf1p kinases. Incubation of the CaMKKβ yeast strain with a chemical library screened for inhibitors of the Ca^{2+}/CaM/CaMKKβ pathway (Figure 1A). Although CaM is essential in yeast, activation of most CaM binding proteins in *Saccharomyces cerevisiae* does not require binding of Ca^{2+} to CaM (*15*). Proteins that require binding of Ca^{2+} to CaM are yeast calcineurin and

†This work was supported by National Institutes of Health Grants GM-33976 and DK-074701 to A.R.M. and by a Duke University Pharmacology Scientist Training Program Fellowship to A.A.S.

*To whom correspondence should be addressed. Phone: (919) 681-6209. Fax: (919) 681-7767. E-mail: means001@mc.duke.edu.

[1]Abbreviations: CaM, calmodulin; CaMK, calmodulin-dependent kinase; CaMKK, CaMK kinase; ITC, isothermal titration calorimetry; TFP, trifluoperazine; ΔH, enthalpy change; ΔS, entropy change; ΔC_p, heat capacity change; K_a, affinity constant.

 Published on Web 04/14/2010

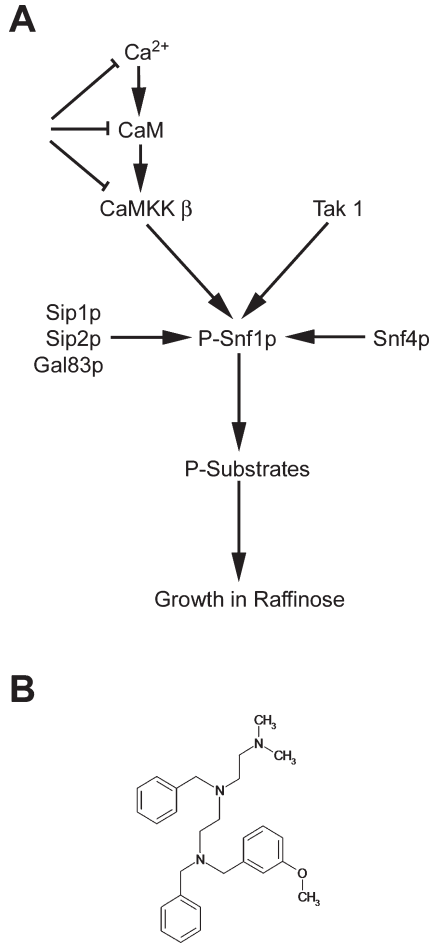

FIGURE 1: Screening for compounds that inhibit the Ca^{2+}/CaM/CaMKKβ pathway in yeast. (A) Strategy for a yeast-based high-throughput screening based on the capability of CaMKKβ to replace the three endogenous Snf1p activators and support yeast growth when raffinose is the major carbon source. See the explanation in the introductory section. Abbreviations: CaMKKβ, rat calmodulin-dependent kinase kinase β; Tak 1, mouse MAPKKK7; Sip1p, Sip2p, and Gal83p, yeast AMPK β subunits; Snf4p, yeast AMPK γ subunit; Snf1p, yeast AMPK α subunit; P-substrates, proteins phosphorylated by Snf1p; arrows, activation steps; flat arrows, possible targets of inhibitors specific for the Ca^{2+}-dependent pathway. (B) Chemical structure of *N*,*N*′-dibenzyl-*N*′-[2-(dimethylamino)ethyl]-*N*-(3-methoxybenzyl)ethylenediamine, henceforth named 125-C9.

yeast calmodulin-dependent kinases Cmk1p and Cmk2p (*16*). None of them are required for yeast viability under standard laboratory conditions, so inhibition of Ca^{2+}/CaM does not affect growth in control yeast (*17*). In addition, yeast expresses several Ca^{2+} channels that in most cases are equivalent to animal Ca^{2+} channels in terms of localization, function, and regulation (reviewed in ref *18*). Therefore, compounds from the library that inhibit CaMKKβ-dependent growth of yeast in raffinose in our screen are expected to target CaMKKβ, CaM, or Ca^{2+} channels.

EXPERIMENTAL PROCEDURES

Chemical Library Screening. The YPR1 yeast strain with three drug sensitizing mutations (Δerg6, Δpdr5, and Δsnq2; LEU2, TRP1, HIS6, MATα) (*19*) was obtained from J. D. York (Duke University Medical Center). Additional deletion of Sak1, Tos3, and Elm1 yeast genes was completed using Guldener's method (*20*). The primers designed to create the loxP-Kan-loxP constructs specific for each gene disruption cassette are 5′-TATAGATTAAGATAAAACGAAAAGAAGCATATTAATAAGGAGTTTTGAACCCAGCTGAAGCTTCGTACGC and 5′-TTAACATCGTAGTCCGATGGAAATTACTTTGAATTTTACACGCATAGGCCACTAGTGGATCTG for Sak1, 5′-GCGCACATATTCTGCATATAAAAAGGAAGCTTTGAAGAATCCAGCTGAAGCTTCGTACGC and 5′-TCATATATTACATCTATTAAAATAATTTACATATATCATGGCATAGGCCACTAGTGGATCTG for Tos3, and 5′-ATAGATATTATTTTTTGAACGCCAGGTTAACAATAATTACTTAGCATGAACCAGCTGAAGCTTCGTACGC and 5′-CGATTATCAGCTAACCCAATCCGACAGATATCATCCTGTAGTTTCATGCATAGGCCACTAGTGGATCTG for Elm1. Expression of flag-rat Camkk2 in yeast was driven by the Cu-inducible yeast vector pCu416CUP1 (*21*), obtained from D. J. Thiele (Duke University Medical Center), and expression of HA-mouse Tak1 was driven by the yeast vector pMM25 (*7*), obtained from M. Carlson (Columbia University, New York, NY). Both vectors contain URA as a marker. In preparation for the screening process, YPR1 ΔSak1, ΔTos3, ΔElm1 yeast was transformed with either the pCu416CUP1 Camkk2 vector or the pMM25 Tak1 vector and grown in URA selective medium (SC -ura, yeast nitrogen base without amino acids, 2% glucose). Both Prestwik (880 compounds) and PPD-Discovery (10057 compounds) chemical libraries were screened in this study. Each library contained compounds in DMSO at a concentration of 1 mM that were added to yeast culture wells at a final concentration of 10 μM. For the screening process, yeast was seeded in liquid medium containing raffinose as the main source of carbon (SC -ura mix, yeast nitrogen base without amino acids, 2% raffinose, 2 mg/mL antimycin) at a low density (650 cells/μL), and these low-density yeast cells were subsequently placed in aliquots of 200 μL per well in 96-well plates, followed by the injection of 2 μL of compound in DMSO (from the aforementioned chemical libraries) per well and incubation at 30 °C for 48 h. In each 96-well plate, we had the following controls: 2 μL of DMSO, which allows yeast growth; 0.5 μM radicicol, which inhibits the growth of yeast in response to Tak1 but not Camkk2; and 5 μM radicicol, which inhibits growth of yeast in response to Tak1 or Camkk2. Yeast growth was monitored 48 h after addition of drugs by optical density measurements (OD) at 600 nm. Any well with $<25\%$ OD versus DMSO control wells was considered growth-inhibited.

Synthesis of Compound 125-C9. New compound 125-C9 was synthesized as an HCl salt. Details of the synthesis are described in the Supporting Information and shown in Scheme 1S of the Supporting Information.

Kinase Assays. CaMKKβ was purified from HEK-293 cells overexpressing Flag-Camkk2 [from rat (*22*)] using anti-Flag-M2 resin (Sigma) as previously described (*4*); trimeric AMPK (AMPKα1 D139A, without kinase activity and thus the ability to autophosphorylate, β1 and γ1) was expressed and purified from bacteria as previously described (*23*). CaMKKβ kinase assays were performed via addition of Flag-CaMKKβ to the mix at a final concentration of 40 nM, in a reaction previously described (*24*), except that 3.5 μM trimeric AMPK was used as a substrate and a range of 125-C9 concentrations from 0.025 to 10 μM were added. CaMKI was purified from bacteria as GST-CaMKI, and CaMKI activity was assayed via addition of GST-CaMKI to the mix at a final concentration of 12 nM. The reaction took place using ADR-1 peptide as a substrate, as previously described (*25*), except that a range of 125-C9 concentrations from 0.1 to 10 μM were added. CaMKII 1−325 [CaMKII missing only the association domain (New England

Biolabs), and thus without the ability to autophosphorylate] was used to assess inhibition of Ca^{2+}/CaM-dependent CaMKII activity by 125-C9 in vitro. Truncated CaMKII was added to the reaction mix to a final concentration of 5.5 nM. The reaction proceeded as previously described (*26*), except that a range of 125-C9 concentrations from 0.1 to 10 μM were added. To assess inhibition of CaMKII autonomous activity by 125-C9 in vitro, full-length CaMKII (Calbiochem) was used, allowing for autophosphorylation and thus Ca^{2+}/CaM-independent activity. Full-length CaMKII was initially autophosphorylated by incubation at 30 °C for 10 min in a solution containing 50 mM HEPES (pH 7.0), 10 mM $MgCl_2$, 100 μM ATP, 1 mM $CaCl_2$, 1 μM CaM, 0.5 mM dithiothreitol, and 0.5 mg/mL BSA. This reaction mixture was then chilled to 4 °C, and inhibition of CaMKII autonomous activity by compound 125-C9 was assessed by addition of autophosphorylated CaMKII to the reaction mix at a final concentration of 3.7 nM in the presence of Ca^{2+} (to monitor total CaMKII activity) or EGTA (to monitor autonomous activity) as previously described (*26*), except that a range of 125-C9 concentrations from 0.1 to 10 μM were added. To assay the ability of 125-C9 to inhibit non-CaM-dependent enzymes, wild-type (WT) trimeric AMPK (WT AMPKα1, -β1, and -γ1) was purified as described previously (*27*). Trimeric AMPK was phosphorylated by CaMKKβ in a reaction mix as described above for the CaMKKβ assay, except that no [γ-^{32}P]ATP was present, CaMKKβ was still bound to Flag-antibody beads, and the reaction continued for 30 min, phosphorylating more than 90% of AMPK. The AMPK phosphorylation was followed by removal of CaMKKβ by centrifugation (12000 rpm for 3 min). Phosphorylated trimeric AMPK was assayed for 125-C9 inhibition via addition of the enzyme to the reaction mix to a final concentration of 6.1 nM, and the reaction proceeded as described elsewhere (*28*) with a range of 125-C9 concentrations from 0.1 to 10 μM. For more details of the kinase assay reactions, see the Supporting Information.

Isothermal Titration Calorimetry. Binding of 125-C9, trifluoperazine, and W-13 to Ca^{2+}/CaM was analyzed by ITC using a VP-ITC instrument (Microcal Instruments) at 25 °C (unless otherwise stated) in 50 mM HEPES buffer (pH 6.95), 150 mM KCl, and 2 mM $CaCl_2$. The CaM concentration was 50 μM, whereas the ligand concentration was 3 mM (125-C9, trifluoperazine) or 10 mM (W-13). Using these conditions, ITC experiments yielded plots typified by that in Figure 1S of the Supporting Information, displaying raw power output versus time of 125-C9 injection into the cell containing CaM (top panel) and the corresponding integrated enthalpy changes (ΔH) versus 125-C9:CaM molar ratio. For Ca^{2+}-independent binding analysis, 2 mM $CaCl_2$ was replaced with 2 mM EGTA; all other buffer components remained constant. Heats of dilution were measured via injection of the ligand into the protein-free buffer, and the value obtained was subtracted from the overall heat of reaction to yield the observed heat of binding. Changes in heat capacity (ΔC_p) were obtained from the slope of the plots of ΔH versus temperature after measurement of ΔH for interactions at 15, 25, 45, and 60 °C (*29*). Competition assays were conducted by mixing 50 μM CaM in ITC buffer with the indicated competing agent at the indicated ratios prior to titration with the corresponding CaM antagonist. Proton transfers were assessed using 50 mM HEPES, 50 mM cacodylate, 50 mM MOPS, or 50 mM Tris buffer at pH 6.95 with 150 mM KCl and 2 mM $CaCl_2$. The number of released protons was obtained from the slope of the plot of $\Delta H_{observed}$ versus $\Delta H_{ionization}$ (*30*). Data were analyzed using MicroCal Origin version 5.0 and were fitted with the sequential binding model, permitting estimation of the affinity constant (K_a), enthalpy changes (ΔH), entropy changes (ΔS), and stoichiometry (n).

Inhibition of Cell Cycle Re-Entry by CaM Antagonists. WI-38 cells were withdrawn from the cell cycle to the G0 phase by serum starvation and released back into proliferation by addition of 10% fetal bovine serum to the medium as previously described (*31*). 125-C9, TFP, or W-13 was added to culture media simultaneously with 10% fetal bovine serum to stimulate re-entry into the cell cycle. Cells were kept in media for 21 h. After this period, cells were harvested and fixed and their DNA was stained with propidium iodide for analysis of apoptosis and cell cycle phases as previously described (*31*).

RESULTS

Yeast-Based Screening of Chemical Small Libraries. Screens of two small libraries of compounds (Prestwick and PPD Discovery) yielded hundreds of compounds that inhibited yeast growth of both Camkk2 and Tak1 strains, so these compounds were considered either toxic or nonspecific (example in Figure 2S of the Supporting Information). However, a number of compounds preferentially inhibited Camkk2 yeast growth: one compound from the Prestwick library (clomiphene citrate) and nine compounds from the PPD library (see Figure 2S of the Supporting Information). Clomiphene citrate inhibits CaM-dependent CaMKKβ activity in vitro with low affinity at 100 μM (results not shown); moreover, clomiphene citrate has been previously described as a possible CaM inhibitor (*32*) and therefore was not novel. However, none of the nine inhibitory compounds from the PPD library had been previously described. All inhibitors are substituted ethyleneamines, and these compounds inhibit CaMKKβ activity in vitro to various degrees (results not shown). The most potent compound, *N*,*N*′-dibenzyl-*N*′-[2-(dimethylamino)ethyl]-*N*-(3-methoxybenzyl)ethylenediamine, henceforth called 125-C9 (Figure 1B), was selected for further analysis.

Compound 125-C9 Inhibits CaM-Dependent Kinases in Vitro. 125-C9 was synthesized as the hydrochloride salt, as described in the Supporting Information and shown in Scheme 1S of the Supporting Information. This form of the compound is highly soluble in H_2O at ≤pH 7.0 and was used for all subsequent in vitro analysis. We first characterized the ability of 125-C9 to inhibit CaMKKβ activity in vitro. CaMKKβ assays using AMPK (full-length protein) as a substrate showed that compound 125-C9 inhibits CaMKKβ activity in vitro in a dose-dependent manner (Figure 2A). We then determined the mechanism by which the compound inhibits CaMKKβ with kinase assays with various concentrations of several components: ATP, substrate (AMPK), and CaM. Variations in ATP and substrate concentration did not alter the kinetics of inhibition of CaMKKβ by 125-C9 (results not shown). However, increased concentrations of CaM displaced the inhibitory curve of 125-C9 to the right (Figure 2A). The estimated IC_{50} value of 125-C9 ranged from 4.6 to 260 μM depending on the CaM concentration in the assay (see Table 1S of the Supporting Information for IC_{50} values obtained for CaMKKβ with different CaM concentrations). These results indicate that 125-C9 inhibits CaMKKβ competitively with CaM.

We tested the specificity of 125-C9 for CaMKKβ in vitro by monitoring its ability to inhibit the activity of other CaM-dependent kinases. We found that 125-C9 also inhibits CaMKKα activity (the other member of the CaMKK subfamily)

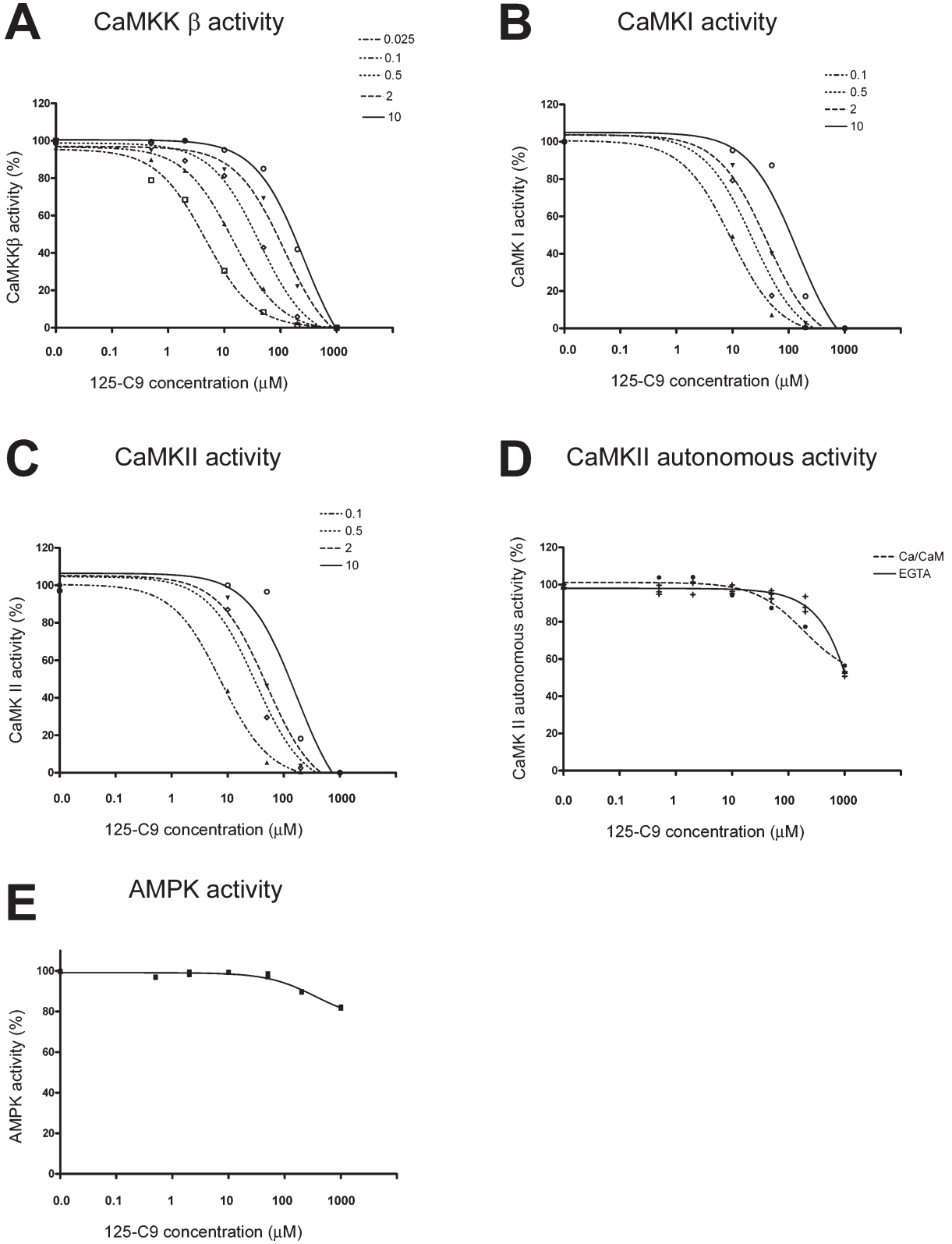

FIGURE 2: Kinase assays in vitro. Newly synthesized 125-C9 was tested for its ability to inhibit the Ca^{2+}/CaM-dependent activity of CaMKKβ (A), CaMKI (B), or CaMKII (C), as well as its ability to inhibit the autonomous (Ca^{2+}/CaM-independent) activity of preautophosphorylated CaMKII (D), and the activity of the Ca^{2+}/CaM-independent enzyme AMPK (E). For all the Ca^{2+}/CaM-dependent assays, CaM was used at a range of concentrations {0.1 (▲), 0.5 (◇), 2 (▼), and 10 μM (○) [and also at 0.025 μM (□) for CaMKKβ]}, as indicated in panels A−C. For CaMKII autonomous activity, CaMKII was preincubated with Ca^{2+}/CaM for 10 min before the reaction was started via the addition of either compound 125-C9, [γ-^{32}P]ATP, substrate peptide, and the Ca^{2+} chelator EGTA (solid line) or compound 125-C9, [γ-^{32}P]ATP, substrate peptide, and Ca^{2+}/CaM (dashed line), as indicated in panel D. For details of the kinase reactions, see Experimental Procedures.

in a CaM-competitive manner (results not shown). As the inhibition in both cases is competitive with respect to CaM, we tested the inhibitory ability of 125-C9 on other CaM-dependent enzymes such as CaMKI and CaMKII. Although normally CaMKI must be activated by phosphorylation at T177 by a CaMKK, it phosphorylates the substrate peptide ADR1 equally

well without such activation (*25*). To avoid misinterpretations due to the effect of 125-C9 on CaMKKs, the analysis of 125-C9 was performed on unphosphorylated CaMKI using ADR1 as the substrate. The results show that 125-C9 also inhibits CaMKI in a CaM-competitive manner (Figure 2B). In addition, 125-C9 inhibits CaMKI activity in a CaM-competitive manner when CaMKI is preactivated by CaMKKβ with synapsin site I peptide as the substrate (results not shown). Similar to CaMKKβ and CaMKI, 125-C9 also inhibits CaMKII activity in a CaM-competitive manner using autocamtide-2 as the substrate (Figure 2C). These results reveal that 125-C9 inhibits several CaM-dependent kinases.

This observation led us to question whether 125-C9 inhibits only CaM-dependent kinase activity. We tested this idea using two different enzymes: a CaMK that is no longer dependent on CaM and a kinase that does not belong to the CaMK family. In the first case, we used autophosphorylated CaMKII, since autophosphorylated CaMKII has Ca^{2+}/CaM-independent activity (*33*). Full-length CaMKII was first incubated for 10 min in the presence of unlabeled ATP to increase the level of autophosphorylation and subsequently was incubated with a range of concentrations of 125-C9, substrate autocamtide-2, labeled ATP, and EGTA to demonstrate its Ca^{2+}/CaM-independent activity. As predicted, autophosphorylation induced autonomous activity, since EGTA activity was shown to be almost equal to Ca^{2+}/CaM activity (Figure 2D, at a 125-C9 concentration of 0 μM). Importantly, 125-C9 no longer inhibited CaMKII activity, since high concentrations of the compound (100−1000 μM) have an only minimal effect on autophosphorylated CaMKII activity in the presence of either Ca^{2+}/CaM or EGTA (Figure 2D). In the second case, we used AMPK as a kinase that does not belong to the CaMK family. The kinase activity of AMPK is not inhibited by 125-C9 as shown by in vitro activity assays (Figure 2E). These results indicate that 125-C9 inhibits only CaM-dependent kinase activity and does not affect kinases with activity independent of CaM.

125-C9 Binds Directly to CaM. We performed ITC to determine whether 125-C9 binds CaM-dependent kinases (for example, CaMKI), or CaM itself. Injection of 125-C9 into the cell containing the CaMKI sample gave no binding signal (Figure 3S of the Supporting Information), indicating that there was no direct binding of 125-C9 to CaMKI. However, binding of 125-C9 to CaM was clearly demonstrated in the presence of Ca^{2+} (Figure 3A and Figure 1S of the Supporting Information). The best fitting curve for such a profile was obtained using the sequential binding model (Origin version 5.0); we tested models for binding different stoichiometries of 125-C9 and calmodulin and monitored the quality of the fit by χ^2 values (Table 2S of the Supporting Information). The χ^2 value reached a minimum for curves fitting five or more binding sites, suggesting that five molecules of 125-C9 bind one molecule of CaM. The association constants for the five binding sites under our experimental conditions using HEPES buffer ranged from 3.32×10^6 M^{-1} for the highest-affinity site to 5.8×10^3 M^{-1} for the lowest-affinity site (Table 1). On the basis of our data, the dissociation constant values for the first two molecules of 125-C9 binding to CaM are 1.4 and 0.3 μM, respectively, which are consistent with 125-C9 inhibition of CaM/CaMK activity at low micromolar concentrations (Figure 2 and Table 1).

Additionally, since CaM binding to most CaM-dependent enzymes and CaM antagonists is dependent on Ca^{2+}, we tested whether 125-C9 binds CaM in the absence of Ca^{2+} and in the presence of the Ca^{2+} chelator EGTA. Under these conditions, 125-C9 did not bind CaM (Figure 3B), indicating that binding of 125-C9 to CaM is absolutely dependent on Ca^{2+}.

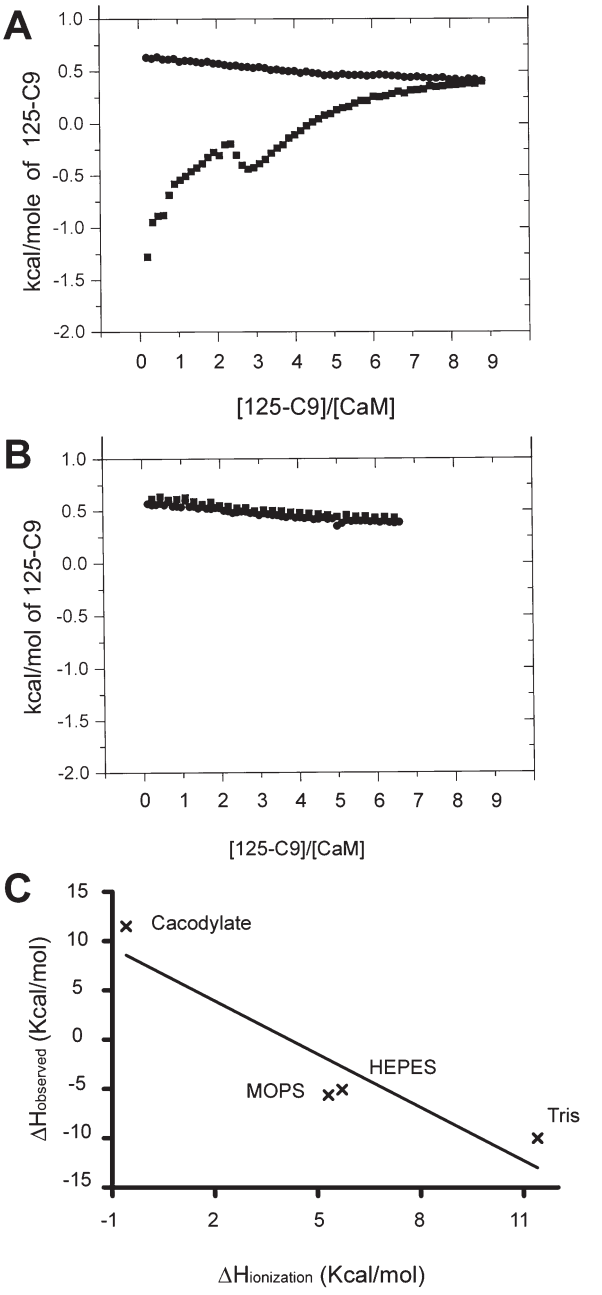

FIGURE 3: Isothermal titration calorimetry of CaM with compound 125-C9. Representative plot of enthalpy changes for CaM [50 μM (■)] or buffer without CaM (●) as compound 125-C9 is injected into the cell in the presence of Ca^{2+} [2 mM (A)] or in the absence of Ca^{2+} [EGTA at 2 mM (B)]. (C) Plot showing the observed enthalpy change ($\Delta H_{observed}$) vs the enthalpy of ionization ($\Delta H_{ionization}$) for each buffer used in ITC analysis of compound 125-C9 binding to CaM at neutral pH (pH 6.95). The line represents the linear least-squares best fit ($R^2 = 0.87$; slope = −1.8; $\Delta H_{observed} = 7.5 \pm 3.4$ kcal/mol when $\Delta H_{ionization} = 0$).

Binding of 125-C9 to CaM in HEPES buffer results in an overall favorable observed entropy [ΔS (see Table 3S of the Supporting Information)], derived from favorable entropies of binding at each site (Table 1). 125-C9 binding also results in a small favorable observed enthalpy [$\Delta H_{observed}$ (Table 3S of the Supporting Information)], the summation of favorable and unfavorable enthalpies at individual binding sites (Table 1).

Table 1: ITC-Estimated Parameters for Binding of Compound 125-C9 to Calmodulin in HEPES Buffer

site	K_a (M^{-1})	ΔH_{obs} (kcal mol^{-1})	ΔS (kcal mol^{-1} K^{-1})
1	$(7.3 \pm 0.6) \times 10^5$	-3.1 ± 0.1	0.017
2	$(32.9 \pm 2.5) \times 10^5$	0.82 ± 0.1	0.033
3	$(4.0 \pm 0.2) \times 10^4$	-1.9 ± 0.1	0.015
4	$(6.3 \pm 0.7) \times 10^3$	-1.5 ± 0.2	0.012
5	$(5.8 \pm 0.7) \times 10^3$	0.7 ± 0.2	0.019

Since $\Delta H_{observed}$ is the result of several factors, including binding enthalpy ($\Delta H_{binding}$) and the transfer of a proton between the complex and buffer, we could not conclude from these data alone whether the binding of 125-C9 to CaM is also accompanied by a favorable binding enthalpy. However, we will address this issue below. A favorable entropy upon binding of 125-C9 to CaM contrasts with the cases of other well-known CaM antagonists such as TFP and W-13, whose binding to CaM is basically mediated by favorable enthalpy only (refs *34* and *35* and Table 3S of the Supporting Information).

To determine the contribution from the heat of ionization, we analyzed binding of 125-C9 with CaM using four buffers with differing heats of ionization ($\Delta H_{ionization}$): cacodylate (−0.6 kcal/mol), MOPS (5.3 kcal/mol), HEPES (5.7 kcal/mol), and Tris (11.4 kcal/mol) (*36*). The slope of the plot of $\Delta H_{observed}$ versus $\Delta H_{ionization}$ indicates that binding of 125-C9 to CaM results in the loss of two protons by the complex (Figure 3C). As shown in Figure 3C, binding of 125-C9 to CaM changes from an exothermic reaction to an endothermic one in a buffer-dependent manner. The estimated $\Delta H_{binding}$ in an ideal buffer with a null heat of ionization is 7.5 ± 3.4 kcal/mol, indicating that binding is actually endothermic. Therefore, binding of 125-C9 to CaM is driven solely by entropy, since $\Delta H_{binding}$ is endothermic, and results in the release of two protons.

Compound 125-C9 Binds CaM at Overlapping Sites for TFP and W-13. Because 125-C9 binds CaM with affinities similar to those of classic CaM antagonists such as trifluoperazine (TFP) and W-13, we performed ITC competition assays to assess whether the CaM sites that bind 125-C9 are unique or overlap with the binding sites of these other compounds. On the basis of ITC analysis, TFP has been previously shown to bind CaM at a ratio of 5:1 (TFP:CaM) (ref *34* and our results). Our titrations suggest that 125-C9 binds CaM at five sites in the absence of TFP, as mentioned above (Table 1 and Figure 4A). However, 125-C9 binds CaM at three sites with a 2:1 TFP:CaM ratio; 125-C9 binds CaM at one site with a 5:1 TFP:CaM ratio, with a K_a value of 0.53×10^5 M^{-1}, and 125-C9 does not bind CaM with a 10:1 TFP:CaM ratio (Figure 4A). The reverse experiment shows that TFP does not bind CaM when injected into 5:1 or 10:1 125-C9:CaM mixtures (Figure 4B). These results are consistent with a model of binding for 125-C9 in which all five binding sites are shared between 125-C9 and TFP, and binding occurs with similar affinities for both compounds. On the other hand, W-13 has been shown to bind CaM at a 2:1 W-13:CaM ratio (ref *35* and our observations), and we repeated the experiments described above with several W-13:CaM ratios. Compound 125-C9 injected into a 1:1 W-13/CaM mixture binds to CaM at four sites (Figure 4A); the same result was obtained when compound 125-C9 was injected into a 2:1 W-13/CaM mixture and a 5:1 W-13/CaM mixture. However, at the highest concentration of W-13, binding of 125-C9 to CaM occurs with lower affinity, as reflected by changes in K_a values for the three highest-affinity CaM binding sites from $(7.3 \pm 0.6) \times 10^5$, $(32.9 \pm 2.5) \times 10^5$, and $(4.1 \pm 0.3) \times 10^4$ M^{-1} without competition to $(9.0 \pm 0.9) \times 10^5$, $(2.2 \pm 0.2) \times 10^5$, and $(9.8 \pm 0.7) \times 10^3$ M^{-1} with W-13 competition, respectively (Table 4S of the Supporting Information). The reverse experiment, preincubating CaM with 125-C9 and injecting W-13, shows that W-13 injected into the 5:1 125-C9/CaM mixture loses one binding site and binds to the other with decreased affinity (changes K_a values from $(8.0 \pm 1.1) \times 10^4$ and $(1.2 \pm 0.2) \times 10^4$ M^{-1} without competition to $(1.6 \pm 0.1) \times 10^3$ M^{-1} with 125-C9 competition (Figure 4C and Table 4S of the

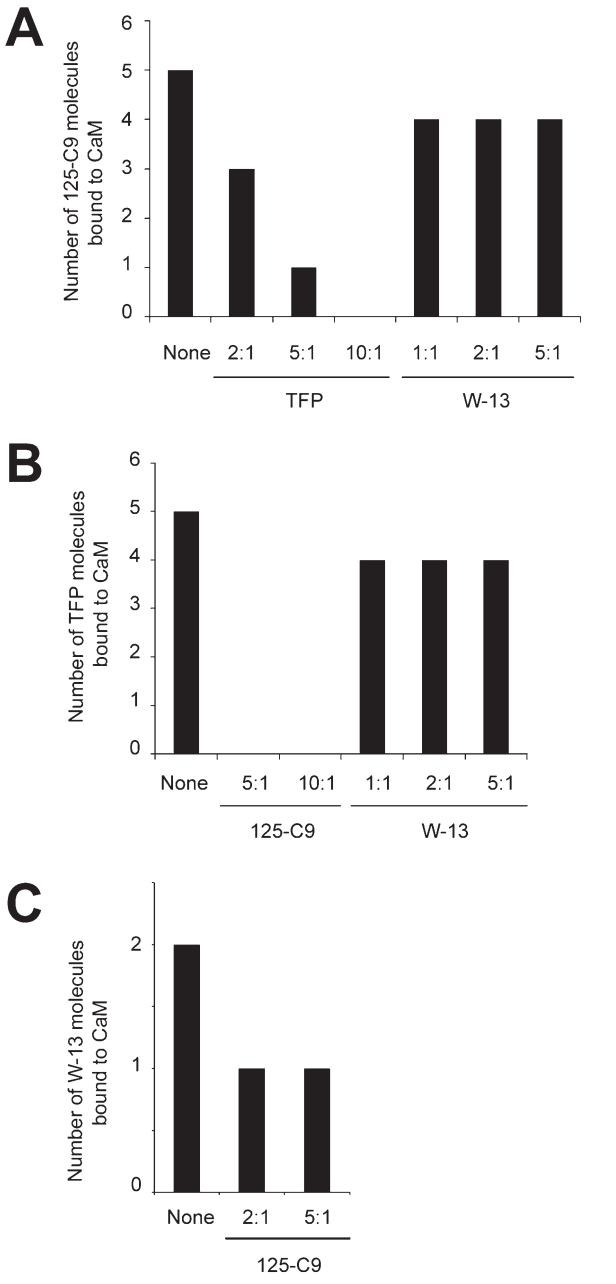

FIGURE 4: Binding of CaM antagonists to CaM preincubated with a different CaM antagonist. (A) Number of 125-C9 molecules bound to CaM without competition (none), CaM preincubated with TFP at ratios of 2:1, 5:1, and 10:1 (TFP:CaM), or CaM preincubated with W-13 at ratios of 1:1, 2:1, and 5:1 (W-13:CaM), as indicated. (B) Number of TFP molecules bound to CaM without any competition (none), CaM preincubated with 125-C9 at ratios of 5:1 and 10:1 (125-C9:CaM), or CaM preincubated with W-13 at ratios of 1:1, 2:1, and 5:1 (W-13:CaM), as indicated. (C) Number of W-13 molecules bound to CaM without any competition (none) or CaM preincubated with 125-C9 at ratios of 2:1 and 5:1 (125-C9:CaM), as indicated.

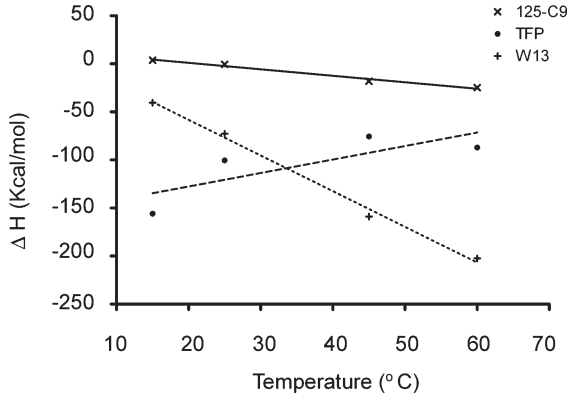

FIGURE 5: Heat capacity changes for CaM binding antagonists 125-C9, TFP, and W-13. Enthalpy values (ΔH) vs temperature (15−60 °C) plotted for compound 125-C9, TFP, and W-13 as indicated, with the linear least-squares best fit for each CaM antagonist. R^2 values are 0.983, 0.784, and 0.994 for 125-C9, TFP, and W13, respectively. See Table 2 for additional information.

Supporting Information). The same results were obtained when W-13 was injected into the 2:1 125-C9/CaM mixture, suggesting that the first two molecules of 125-C9 that bind to CaM compete for the same sites in CaM that bind W-13 (Figure 4C). As a control, we monitored the competition between TFP and W-13 by preincubating W-13 with CaM and injecting TFP. The results indicate that, similar to 125-C9, TFP competes with W-13 for at least one binding site (Figure 4B) and binds to the other sites with lower affinity, as reflected by the change in K_a values for the three best CaM binding sites from $(1.3 \pm 0.1) \times 10^5$, $(1.0 \pm 0.1) \times 10^5$, and $(3.4 \pm 0.2) \times 10^4$ M^{-1} without competition to $(3.3 \pm 0.2) \times 10^4$, $(2.3 \pm 0.1) \times 10^4$, and $(1.1 \pm 0.1) \times 10^4$ M^{-1} with W-13 competition, respectively (Table 4S of the Supporting Information). Overall, these results are consistent with a model of binding in which 125-C9 and W-13 compete for common sites in CaM and TFP also competes with W-13 for common sites.

Since there are common CaM binding sites for 125-C9, TFP, and W-13, we sought more information about the mechanism of binding of each compound by measuring the change in heat capacity (ΔC_p). At a low temperature (5 °C), we noticed that binding of the antagonist did not occur (W-13) or occurred at a number of sites smaller than the number observed at higher temperatures (125-C9); therefore, a range of temperatures from 15 to 60 °C was used. TFP shows a positive ΔC_p, although the fit to the data for this compound was poor (Figure 5), suggesting either partial denaturation of the protein or a changing binding mechanism as a function of temperature. On the other hand, W-13 and 125-C9 show negative ΔC_p values with good linear fits (Figure 5 and Table 2). However, the absolute value for W-13 is −3.7 kcal mol^{-1} K^{-1}, much higher than the value for 125-C9 (−0.7 kcal mol^{-1} K^{-1}). Overall, these results add to the previously discussed evidence that TFP, W-13, and 125-C9 may have different mechanisms for binding CaM.

125-C9 Enters into Cells and Inhibits Re-Entry of G0 Cells into the Cell Cycle. Because 125-C9 binds to CaM with an affinity comparable to that of TFP and W-13, we tested whether it would inhibit a CaM-dependent process in living cells in a comparable way. For this purpose, we monitored the effect of 125-C9 on cell cycle re-entry of quiescent cells, as CaM plays a primary role in this process. We tested 125-C9 on WI-38, a human cell line previously used to study the role of CaM in the transition from quiescence into cell proliferation (*37*). In a

Table 2: Heat Capacity Changes for CaM Binding Antagonists 125-C9, TFP, and W-13

compound	ΔC_p (kcal mol^{-1} K^{-1})	deviation from 0 (P value)
125-C9	-0.674 ± 0.0633	0.0087[a]
TFP	1.402 ± 0.528	0.0768
W-13	-3.709 ± 0.200	0.0029[a]

[a] P values for deviation from 0 are significant.

preliminary experiment, 10 μM 125-C9 prevented an increase in the number of WI-38 cells during a 4 day incubation, but after the antagonist had been washed away, cells resumed their growth (results not shown). This result indicates that the inhibitory effect of 125-C9 is reversible, which has been shown for TFP and W-13 (*31*, *38*, *39*). We used concentrations of TFP of up to 15 μM and concentrations of W-13 of up to 30 μM based on toxicity concerns, because these doses have been previously shown to almost completely inhibit cell proliferation but not pose a toxicity threat (*31*, *38*, *39*). Because of the similarities between 125-C9 and TFP in binding CaM, we chose a similar range of concentrations for 125-C9. First, we tested the survival of WI-38 cells with 21 h CaM antagonist incubations. The toxicity of the compounds tested is shown in Figure 6A: 125-C9 induces apoptosis in 9.6% of the cell population at 15 μM, while it does not induce apoptosis at 10 μM (0.71%, based on fragmented DNA). Similarly, TFP shows only background apoptosis at both 10 and 15 μM, while W-13 also shows background apoptosis up to 30 μM. These results indicate that 125-C9 can be safely used in mammalian cell lines for periods of time of 21 h at concentrations of up to 10 μM.

To test the ability of 125-C9 to inhibit cell proliferation at 10 μM, the effect of 125-C9 on quiescent WI-38 cells stimulated to re-enter the cell cycle was analyzed. 125-C9 blocks cells in the G1 phase at 10 μM, as shown by the increase in number of cells in the G1 phase from 70% in untreated control cells to 92% in 125-C9-treated cells (Figure 6B). This effect is similar to that of TFP at 15 μM and W-13 at 30 μM (Figure 6B). All three CaM antagonists prevent the transition into the S phase, as shown by a decrease in the population in the S phase from 7% in untreated cells to 2−3% in antagonist-treated cells (Figure 6C) and a decrease in the population in the G2 and M phases from 22% in untreated cells to 4−6% in antagonist-treated cells (Figure 6D). In conclusion, 125-C9 inhibits CaM in cells in a manner similar to, but slightly better than, that of TFP and W-13.

DISCUSSION

In this study, we successfully used a simple high-throughput yeast strategy to screen two libraries of compounds and identified the compound with the highest affinity for CaM as 125-C9. Additionally, we identified specific similarities and differences between 125-C9 and two of the best characterized CaM antagonists, TFP and W-13. The approach presented here can be applied to larger libraries and to proteins other than those in the CaMKKβ pathway.

This approach is successful because our gene of interest (CaMKKβ) is part of an evolutionarily conserved pathway among eukaryotic cells [the snf1p/AMPK pathway (*9*)]. In addition, our method is simple because only a small number of controls are required. These controls are (a) an alternative activator of snf1p different enough from the protein of interest to distinguish specific inhibitors from nonspecific inhibitors, (b) a known inhibitor compound to test each plate for drug sensitivity,

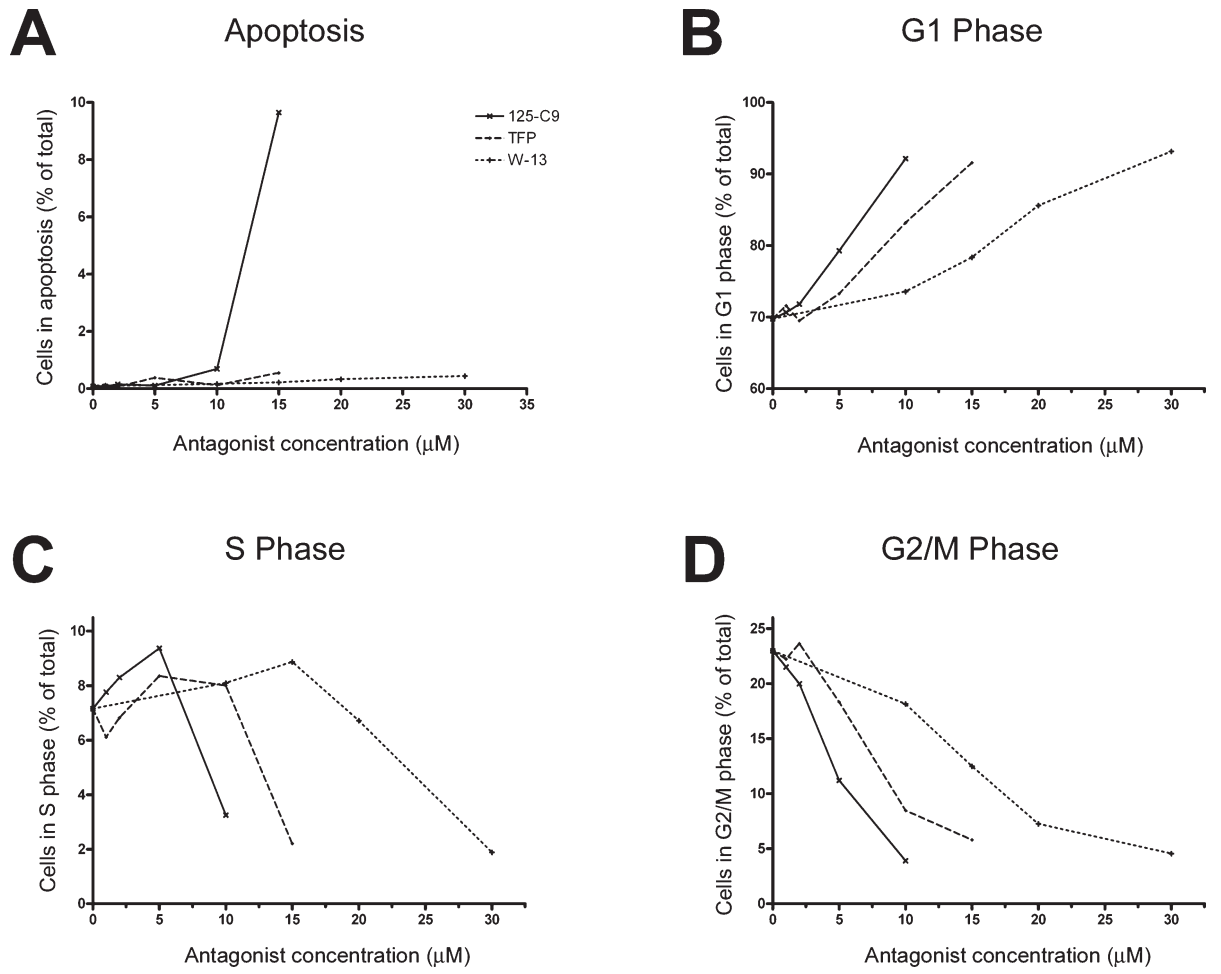

FIGURE 6: Effects of CaM antagonists on apoptosis and block of re-entry into the cell cycle of cells in the G0 phase. WI-38 cells were driven into the G0 phase using medium with 0.5% FBS for 26 h and then stimulated to re-enter the cell cycle with 10% FBS in medium for 21 h, in the presence of the indicated CaM antagonist. Then cells were trypsinized, fixed, stained with propidium iodide, and monitored by flow cytometry to determine the percentage of cells in apoptosis (A), G1 phase (B), S phase (C), and G2 and M phases (D).

and (c) vehicle alone. In our study, we used TAK1 as the alternative activator because it is a mammalian activator like CaMKKβ but is not Ca^{2+}/CaM-dependent. We used radicicol as the inhibitor control and DMSO as the vehicle in each 96-well plate because radicicol has been described as a selective TAK1 inhibitor (*40*), and DMSO is the vehicle for the compounds in the chemical libraries. Finally, we had a drug-sensitized yeast strain available to allow enough inhibitor inside the yeast cells, thereby increasing the sensitivity of the assay. Moreover, using cell growth as the indicator (monitored by the optical density at 600 nm) contributes to the simplicity of the screening process. Although it is not the first time that yeast, with more sophisticated experimental designs, has been used for screening purposes [for example, screening for aptamers that regulate transcription by transfecting yeast with a library of constructs containing GFP linked to the aptamers (*41*)], to the best of our knowledge this is the first time this strategy has been used to screen a library of small molecules. We suspect we did not find any inhibitors that directly target CaMKKβ because of the limited number of compounds (<11000) in the chemical libraries. However, the strategy has been proven to be successful since the assay has produced effective inhibitors for the CaMKKβ activator CaM.

125-C9 directly binds to CaM to inhibit CaM-dependent enzymes as shown by our ITC experiments and in vitro kinase assays. Unlike binding of antagonists TFP and W-13 to CaM (*34*, *35*) (and Table 3S of the Supporting Information), binding of 125-C9 to CaM is not enthalpy-driven, since $\Delta H_{binding}$ is unfavorable, at least near room temperature. Instead, binding of 125-C9 to CaM is driven by entropy, which suggests the interaction is due mostly to hydrophobic interactions. This is supported by the loss of two protons we observe during binding at pH 6.95, a loss consistent with a decrease in polarity and an accompanying shift in pK_a. Moreover, protonation changes during an interaction are consistent with the observed decrease in water solubility (thus, increased hydrophobicity) of compound 125-C9 at higher pH values. As stated in Results, at pH ≥ 7, 125-C9 becomes less soluble in water, which predicts a favorable interaction with the hydrophobic pockets of CaM. The negative slope of the plot of $\Delta H_{observed}$ versus $\Delta H_{ionization}$ indicates that the 125-C9−CaM complex loses two protons, which is consistent with the protonation of 125-C9 at slightly acidic pH values before formation of the complex. The two protons released by the complex most likely do not come from CaM because at neutral pH only histidine (pI 7.59) is thought to release protons and CaM has only one histidine residue. On the other hand, 125-C9 contains three amines (Figure 1C) that would be predicted to be protonated at the pH used in this study (pH 6.95), and the loss of two of these charges upon interaction with CaM would facilitate favorable hydrophobic interaction. Interestingly, compound 125-C9 seems to be different from all peptides analyzed so far in that its interaction with CaM results in the release of two protons. Indeed, binding of peptides derived from different

CaM-dependent proteins, such as smMLCK, melittin, and CaMKII, results in no change in protonation (*42*−*44*). Therefore, binding of 125-C9 to CaM is driven by entropy, consistent with the loss of positive charges of 125-C9 upon binding and the consequent increase in hydrophobicity.

An interaction driven by favorable entropy is often associated with the release of H_2O from the surface, an event that has been previously shown to occur during several peptide−CaM binding interactions displaying negative ΔC_p values (*45*). Our results suggest that the mechanism of binding of 125-C9 to CaM shares some similarities with the mechanism of binding of peptide to CaM but that the mechanisms of TFP and W-13 do not. In a fashion similar to that for binding of peptide to CaM, binding of 125-C9 to CaM results in a negative ΔC_p with a magnitude similar to that of peptide binding [the value of 0.67 ± 0.06 kcal mol^{-1} K^{-1} for binding of 125-C9 to CaM is similar to the value of 0.76 ± 0.12 kcal mol^{-1} K^{-1} for binding of peptides derived from CaMKI, nitric oxide synthase, and melittin to CaM (*45*)]. Interestingly, the ΔC_p for W-13 is much larger, indicating that the binding mechanism of W-13 and CaM may be different from that of 125-C9 and CaM. On the other hand, we did not obtain a good fit for the ΔC_p of TFP, possibly due to the fact that the central helix of CaM (residues 73−77) partially unwinds to form a loop at >25 °C, an event previously inferred from differential scanning calorimetry studies (*42*). A similar situation has been described for the CaM binding smMLCK peptide, for which ΔH decreases linearly relative to temperature increases only up to 25 °C, but linearity is lost as the temperature increases to 35 °C (*42*). This observation also suggests that W-13 does not contact the central helix of CaM [similar to the previously observed binding between W-7 and CaM (*46*)] and that 125-C9 possibly does not interact with the central helix in the same way TFP does.

Although structural studies would be necessary to confirm these results, our data are consistent with 125-C9 binding CaM at five different sites. χ^2 values decrease consistently as the stoichiometry of the sequential binding sites model is increased from one to five in HEPES buffer (Table 2S of the Supporting Information) as well as cacodylate, MOPS, and Tris buffers (results not shown). In addition, a model of six binding sites does not further improve fitting on the basis of χ^2 values, indicating that the five-binding site model is optimal. Binding parameters such as association enthalpy and entropy change only slightly from a model of four binding sites to one of five binding sites. Although we are confident of the stoichiometry, given the large number of variables and limited number of data points for an ITC curve (typically 58 injections per experiment), the curve fitting is underdetermined. Thus, the tabulated K_a and ΔH values for each molecule of 125-C9 binding to CaM are estimates subject to considerable error and should not be overinterpreted.

We believe TFP and 125-C9 bind CaM at overlapping sites on the basis of three observations. First, the competition is dose-dependent. Second, the reverse competition experiment (CaM preincubation with 125-C9 and subsequent injection of TFP) prevents binding of TFP to any sites. Third, W-13, which likely shares two binding sites with TFP, also prevents binding of 125-C9 to CaM at one site and decreases the affinity of 125-C9 for another site. Since the published crystal structures indicate that the hydrophobic rings of phenothiazines (TFP) and naphthalenesulfonamides (W-7) interact with the two hydrophobic pockets of CaM (*46*, *47*), it is not surprising that 125-C9, which contains aromatic rings, competes with both TFP and W-13 for binding to CaM at the hydrophobic pockets. Indeed, the competition assays favor a model for binding of CaM to 125-C9 with five sites, including the two hydrophobic pockets in which W-7 and TFP bind. On the basis of the crystal structure, W-7 binds to CaM at two particular sites: the C-terminal hydrophobic and the N-terminal hydrophobic pockets (*46*). We assume that W-7 and W-13 bind to CaM in a similar manner, since both are chloronaphthalenesulfonamide-derived compounds, and both bind to CaM at a ratio of 2:1 (antagonist: CaM) with similar affinities as determined by ITC (*35*). Consistent with the model of binding of 125-C9 to CaM we propose, 125-C9 completely displaces binding of W-13 to one hydrophobic pocket and decreases the affinity of W-13 for the other hydrophobic pocket. Nevertheless, ITC alone does not prove that the sites are the same, since the results could also be interpreted as binding of 125-C9 to overlapping sites, or by induction of a change of conformation in CaM upon binding the first molecule of 125-C9 such that binding of W-13 to the other site is prevented. However, two facts support our model of binding of 125-C9 to the two CaM hydrophobic pockets: TFP also binds to the two hydrophobic pockets on the basis of the crystal structure, and our competition assays between TFP and W-13 show a parallel with the competition between 125-C9 and W-13.

Two major features are required for a compound to antagonize CaM: a hydrophobic group to interact with the hydrophobic pockets of CaM and a positively charged moiety to interact with negative charges in CaM (*48*, *49*). These two features have been confirmed in both crystal and NMR structures of phenothiazine and naphthalenesulfonamide compounds (*46*, *47*). 125-C9 contains three benzyl rings, accounting for its hydrophobic properties. We propose that either one or two benzyl rings fit into the hydrophobic pocket and establish contacts with hydrophobic residues such as Met 124, Met 144, and Val 136 of the C-terminal pocket, as W-7 and TFP do (*46*, *47*, *50*). 125-C9 also contains three amino groups, which account for positive charges at acidic pH (see the structure in Figure 1). Although upon interaction of 125-C9 with CaM there is a loss of two protons, the remaining protonated amino group may establish electrostatic interactions with side chains from negatively charged residues such as Glu 127, as TFP does (*47*).

125-C9 enters into living mammalian cells and inhibits their proliferation as well as TFP and W-13, as shown by our experiments with cell cycle inhibition. The use of CaM antagonists to inhibit cell proliferation for therapeutic purposes does not seem practical because of the broad range of effects expected from inhibiting a protein with so many functions (*3*). However, the usefulness of CaM antagonists to fight cancer is still a possibility because of the double role of CaM in cancer: cell proliferation and multidrug resistance. Indeed, cancer cells with multidrug resistance have elevated intracellular levels of Ca^{2+} or CaM (*51*), which accelerates the efflux of drug from the cells (*52*). The particular mechanism by which Ca^{2+}/CaM mediates this effect is unknown, but a correlation has been established between inhibition of CaM by different CaM antagonists and multidrug resistance reversal (reviewed in ref *53*). On the other hand, the positive role of CaM in cell proliferation has been widely documented [for example, see the review by Kahl and Means (*37*)]. These studies suggest that the combination of CaM inhibition with other anticancer drug treatments offers a real promise of therapeutic benefits (*53*). Additionally, different CaM antagonists may have different potencies regarding this effect.

In summary, our thermodynamic study demonstrates that 125-C9 directly binds to CaM in a calcium-dependent manner, most likely with a ratio of five molecules of 125-C9 per molecule of CaM. In addition, we have determined that the interaction is entropically driven, with an unfavorable enthalpy of binding near room temperature. This observation and heat capacity studies suggest an important role for hydrophobic interactions during the binding of 125-C9 to CaM. Competition experiments have shown that 125-C9 competes for binding sites with both TFP and W-13 and may bind with similar affinities in conserved sites. Lastly, the differing values of heat capacity for each ligand−protein pair indicate that although binding sites may be conserved, the mechanism of binding is most likely different for each compound.

ACKNOWLEDGMENT

We thank Dr. Milica Moncilovic and Marian Carlson for the Tak1 construct, Dr. John York for discussions regarding the generation of yeast strains, and Dr. James D. Joseph for advice and assistance with screening of the small molecule libraries. We also thank the Duke University Small Molecule Synthesis Facility and Dr. Xin Chen for the synthesis of compound 125-C9.

SUPPORTING INFORMATION AVAILABLE

Extended experimental procedures with a description of the synthesis of 125-C9 (Scheme 1S), an example of ITC raw power output of 125-C9 with CaM (Figure 1S), yeast growth inhibition from the screening process (Figure 2S), ITC analysis of 125-C9 with CaMKI (Figure 3S), summary of IC_{50} values for 125-C9 on different CaMKs (Table 1S), list of χ^2 values for binding of 125-C9 to CaM (Table 2S), summary of thermodynamic parameters for 125-C9, TFP, and W-13 (Table 3S), and summary of K_a values in competition assays (Table 4S). This material is available free of charge via the Internet at http://pubs.acs.org.

REFERENCES

1. Berridge, M. J., Lipp, P., and Bootman, M. D. (2000) The versatility and universality of calcium signalling. *Nat. Rev. Mol. Cell Biol. 1*, 11–21.
2. Chin, D., and Means, A. R. (2000) Calmodulin: A prototypical calcium sensor. *Trends Cell Biol. 10*, 322–328.
3. Yap, K. L., Kim, J., Truong, K., Sherman, M., Yuan, T., and Ikura, M. (2000) Calmodulin target database. *J. Struct. Funct. Genomics 1*, 8–14.
4. Anderson, K. A., Ribar, T. J., Lin, F., Noeldner, P. K., Green, M. F., Muehlbauer, M. J., Witters, L. A., Kemp, B. E., and Means, A. R. (2008) Hypothalamic CaMKK2 contributes to the regulation of energy balance [see comment]. *Cell Metab. 7*, 377–388.
5. Hardie, D. G., Scott, J. W., Pan, D. A., and Hudson, E. R. (2003) Management of cellular energy by the AMP-activated protein kinase system. *FEBS Lett. 546*, 113–120.
6. Shaw, R. J., Lamia, K. A., Vasquez, D., Koo, S. H., Bardeesy, N., Depinho, R. A., Montminy, M., and Cantley, L. C. (2005) The kinase LKB1 mediates glucose homeostasis in liver and therapeutic effects of metformin. *Science 310*, 1642–1646.
7. Momcilovic, M., Hong, S. P., and Carlson, M. (2006) Mammalian TAK1 Activates Snf1 Protein Kinase in Yeast and Phosphorylates AMP-activated Protein Kinase in Vitro. *J. Biol. Chem. 281*, 25336–25343.
8. Hurley, R. L., Anderson, K. A., Franzone, J. M., Kemp, B. E., Means, A. R., and Witters, L. A. (2005) The Ca^{2+}/calmodulin-dependent protein kinase kinases are AMP-activated protein kinase kinases. *J. Biol. Chem. 280*, 29060–29066.
9. Hardie, D. G., Carling, D., and Carlson, M. (1998) The AMP-activated/SNF1 protein kinase subfamily: Metabolic sensors of the eukaryotic cell? *Annu. Rev. Biochem. 67*, 821–855.
10. Nath, N., McCartney, R. R., and Schmidt, M. C. (2002) Purification and characterization of Snf1 kinase complexes containing a defined β subunit composition. *J. Biol. Chem. 277*, 50403–50408.
11. Elbing, K., McCartney, R. R., and Schmidt, M. C. (2006) Purification and characterization of the three Snf1-activating kinases of *Saccharomyces cerevisiae*. *Biochem. J. 393*, 797–805.
12. Sutherland, C. M., Hawley, S. A., McCartney, R. R., Leech, A., Stark, M. J., Schmidt, M. C., and Hardie, D. G. (2003) Elm1p is one of three upstream kinases for the *Saccharomyces cerevisiae* SNF1 complex. *Curr. Biol. 13*, 1299–1305.
13. Hong, S. P., Momcilovic, M., and Carlson, M. (2005) Function of mammalian LKB1 and Ca^{2+}/calmodulin-dependent protein kinase kinase α as Snf1-activating kinases in yeast. *J. Biol. Chem. 280*, 21804–21809.
14. Woods, A., Dickerson, K., Heath, R., Hong, S. P., Momcilovic, M., Johnstone, S. R., Carlson, M., and Carling, D. (2005) Ca^{2+}/calmodulin-dependent protein kinase kinase-β acts upstream of AMP-activated protein kinase in mammalian cells. *Cell Metab. 2*, 21–33.
15. Davis, T. N., Urdea, M. S., Masiarz, F. R., and Thorner, J. (1986) Isolation of the yeast calmodulin gene: Calmodulin is an essential protein. *Cell 47*, 423–431.
16. Cyert, M. S. (2001) Genetic analysis of calmodulin and its targets in *Saccharomyces cerevisiae*. *Annu. Rev. Genet. 35*, 647–672.
17. Geiser, J. R., van Tuinen, D., Brockerhoff, S. E., Neff, M. M., and Davis, T. N. (1991) Can calmodulin function without binding calcium? *Cell 65*, 949–959.
18. Wolfe, D. M., and Pearce, D. A. (2006) Channeling studies in yeast: Yeast as a model for channelopathies? *NeuroMol. Med. 8*, 279–306.
19. Gray, N. S., Wodicka, L., Thunnissen, A. M., Norman, T. C., Kwon, S., Espinoza, F. H., Morgan, D. O., Barnes, G., LeClerc, S., Meijer, L., Kim, S. H., Lockhart, D. J., and Schultz, P. G. (1998) Exploiting chemical libraries, structure, and genomics in the search for kinase inhibitors. *Science 281*, 533–538.
20. Guldener, U., Heck, S., Fielder, T., Beinhauer, J., and Hegemann, J. H. (1996) A new efficient gene disruption cassette for repeated use in budding yeast. *Nucleic Acids Res. 24*, 2519–2524.
21. Labbe, S., and Thiele, D. J. (1999) Copper ion inducible and repressible promoter systems in yeast. *Methods Enzymol. 306*, 145–153.
22. Anderson, K. A., Means, R. L., Huang, Q. H., Kemp, B. E., Goldstein, E. G., Selbert, M. A., Edelman, A. M., Fremeau, R. T., and Means, A. R. (1998) Components of a calmodulin-dependent protein kinase cascade. Molecular cloning, functional characterization and cellular localization of Ca^{2+}/calmodulin-dependent protein kinase kinase β. *J. Biol. Chem. 273*, 31880–31889.
23. Suter, M., Riek, U., Tuerk, R., Schlattner, U., Wallimann, T., and Neumann, D. (2006) Dissecting the role of 5′-AMP for allosteric stimulation, activation, and deactivation of AMP-activated protein kinase. *J. Biol. Chem. 281*, 32207–32216.
24. Tokumitsu, H., Iwabu, M., Ishikawa, Y., and Kobayashi, R. (2001) Differential regulatory mechanism of Ca2^{+}/calmodulin-dependent protein kinase kinase isoforms. *Biochemistry 40*, 13925–13932.
25. Hook, S. S., Kemp, B. E., and Means, A. R. (1999) Peptide specificity determinants at P-7 and P-6 enhance the catalytic efficiency of Ca^{2+}/calmodulin-dependent protein kinase I in the absence of activation loop phosphorylation. *J. Biol. Chem. 274*, 20215–20222.
26. Colomer, J. M., and Means, A. R. (2000) Chronic elevation of calmodulin in the ventricles of trasngenic mice increases the autonomous acivity of calmodulin-dependent protein kinase II, which regulates atrial natriuretic factor gene expression. *Mol. Endocrinol. 14*, 1125–1136.
27. Neumann, D., Woods, A., Carling, D., Wallimann, T., and Schlattner, U. (2003) Mammalian AMP-activated protein kinase: Functional, heterotrimeric complexes by co-expression of subunits in *Escherichia coli*. *Protein Expression Purif. 30*, 230–237.
28. Witters, L. A., and Kemp, B. E. (1992) Insulin activation of acetyl-CoA carboxylase accompanied by inhibition of the 5′-AMP-activated protein kinase. *J. Biol. Chem. 267*, 2864–2867.
29. Cooper, A. (2005) Heat capacity effects in protein folding and ligand binding: A re-evaluation of the role of water in biomolecular thermodynamics. *Biophys. Chem. 115*, 89–97.
30. Jelesarov, I., and Bosshard, H. R. (1999) Isothermal titration calorimetry and differential scanning calorimetry as complementary tools to investigate the energetics of biomolecular recognition. *J. Mol. Recognit. 12*, 3–18.
31. Kahl, C. R., and Means, A. R. (2004) Regulation of cyclin D1/Cdk4 complexes by calcium/calmodulin-dependent protein kinase I. *J. Biol. Chem. 279*, 15411–15419.
32. Musgrove, E. A., Wakeling, A. E., and Sutherland, R. L. (1989) Points of action of estrogen antagonists and a calmodulin antagonist within the MCF-7 human breast cancer cell cycle. *Cancer Res. 49*, 2398–2404.

33. Lou, L. L., Lloyd, S. J., and Schulman, H. (1986) Activation of the multifunctional Ca^{2+}/calmodulin-dependent protein kinase by autophosphorylation: ATP modulates production of an autonomous enzyme. *Proc. Natl. Acad. Sci. U.S.A. 83*, 9497–9501.
34. Makarov, A. A., Tsvetkov, P. O., Villard, C., Esquieu, D., Pourroy, B., Fahy, J., Braguer, D., Peyrot, V., and Lafitte, D. (2007) Vinflunine, a novel microtubule inhibitor, suppresses calmodulin interaction with the microtubule-associated protein STOP. *Biochemistry 46*, 14899–14906.
35. Dagher, R., Brière, C., Fève, M., Zeniou, M., Pigault, C., Mazars, C., Chneiweiss, H., Ranjeva, R., Kilhoffer, M.-C., and Haiech, J. (2009) Calcium fingerprints induced by calmodulin interactors in eukaryotic cells. *Biochim. Biophys. Acta 1793*, 1068–1077.
36. Boyle, M. L. (1999) Titration Microcalorimetry, John Wiley & Sons, Hoboken, NJ.
37. Kahl, C. R., and Means, A. R. (2003) Regulation of cell cycle progression by calcium/calmodulin-dependent pathways. *Endocr. Rev. 24*, 719–736.
38. Grief, F., Soroff, H. S., Albers, K. M., and Taichman, L. B. (1989) The effect of trifluoperazine, a calmodulin antagonist, on the growth of normal and malignant epidermal keratinocytes in culture. *Eur. J. Cancer Clin. Oncol. 25*, 19–26.
39. Chafouleas, J. G., Bolton, W. E., Hidaka, H., Boyd, A. E., and Means, A. R. (1982) Calmodulin and the cell cycle: Involvement in regulation of cell-cycle progression. *Cell 28*, 41–50.
40. Chanmugam, P., Feng, L., Liou, S., Jang, B. C., Boudreau, M., Yu, G., Lee, J. H., Kwon, H. J., Beppu, T., and Yoshida, M. (1995) Radicicol, a protein tyrosine kinase inhibitor, suppresses the expression of mitogen-inducible cyclooxygenase in macrophages stimulated with lipopolysaccharide and in experimental glomerulonephritis. *J. Biol. Chem. 270*, 5418–5426.
41. Suess, B., and Weigand, J. E. (2009) Aptamers as artificial gene regulation elements. *Methods Mol. Biol. 535*, 201–208.
42. Wintrode, P. L., and Privalov, P. L. (1997) Energetics of target peptide recognition by calmodulin: A calorimetric study. *J. Mol. Biol. 266*, 1050–1062.
43. Milos, M., Schaer, J. J., Comte, M., and Cox, J. A. (1987) Microcalorimetric investigation of the interactions in the ternary complex calmodulin-calcium-melittin. *J. Biol. Chem. 262*, 2746–2749.
44. Tse, J. K., Giannetti, A. M., and Bradshaw, J. M. (2007) Thermodynamics of calmodulin trapping by Ca^{2+}/calmodulin-dependent protein kinase II: Subpicomolar Kd determined using competition titration calorimetry. *Biochemistry 46*, 4017–4027.
45. Brokx, R. D., Lopez, M. M., Vogel, H. J., and Makhatadze, G. I. (2001) Energetics of target peptide binding by calmodulin reveals different modes of binding. *J. Biol. Chem. 276*, 14083–14091.
46. Osawa, M., Swindells, M. B., Tanikawa, J., Tanaka, T., Mase, T., Furuya, T., and Ikura, M. (1998) Solution structure of calmodulin-W-7 complex: The basis of diversity in molecular recognition. *J. Mol. Biol. 276*, 165–176.
47. Vandonselaar, M., Hickie, R. A., Quail, J. W., and Delbaere, L. T. (1994) Trifluoperazine-induced conformational change in Ca^{2+}-calmodulin. *Nat. Struct. Biol. 1*, 795–801.
48. Hidaka, H., and Tanaka, T. (1983) Naphthalenesulfonamides as calmodulin antagonists. *Methods Enzymol. 102*, 185–194.
49. Weiss, B., Prozialick, W. C., and Wallace, T. L. (1982) Interaction of drugs with calmodulin: Biochemical, pharmacological and clinical implications. *Biochem. Pharmacol. 31*, 2217–2226.
50. Cook, W. J., Walter, L. J., and Walter, M. R. (1994) Drug binding by calmodulin: Crystal structure of a calmodulin-trifluoperazine complex. *Biochemistry 33*, 15259–15265.
51. Nair, S., Samy, T. S. A., and Krishan, A. (1986) Calcium, calmodulin, and protein content of adriamycin-resistant and -sensitive murine leukemic cells. *Cancer Res. 46*, 229–232.
52. Chen, C. J., Chin, J. E., Ueda, K., Clark, D. P., Pastan, I., Gottesman, M. M., and Roninson, I. B. (1986) Internal duplication and homology with bacterial transport proteins in the mdr1 (P-glycoprotein) gene from multidrug-resistant human cells. *Cell 47*, 381–389.
53. Mayur, Y. C., Jagadeesh, S., and Thimmaiah, K. N. (2006) Targeting calmodulin in reversing multi drug resistance in cancer cells. *Mini Rev. Med. Chem. 6*, 1383–1389.